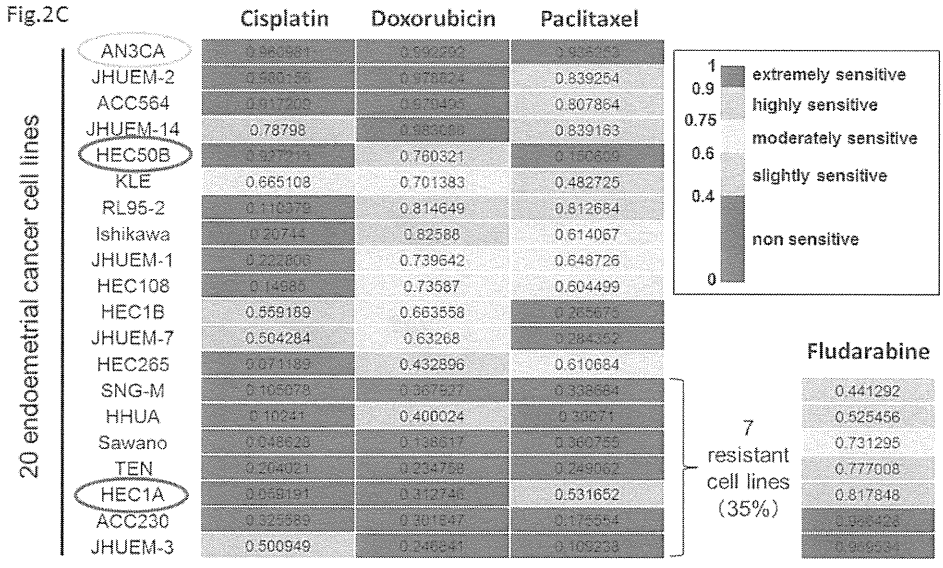

196x120mm (300 x 300 DPI)

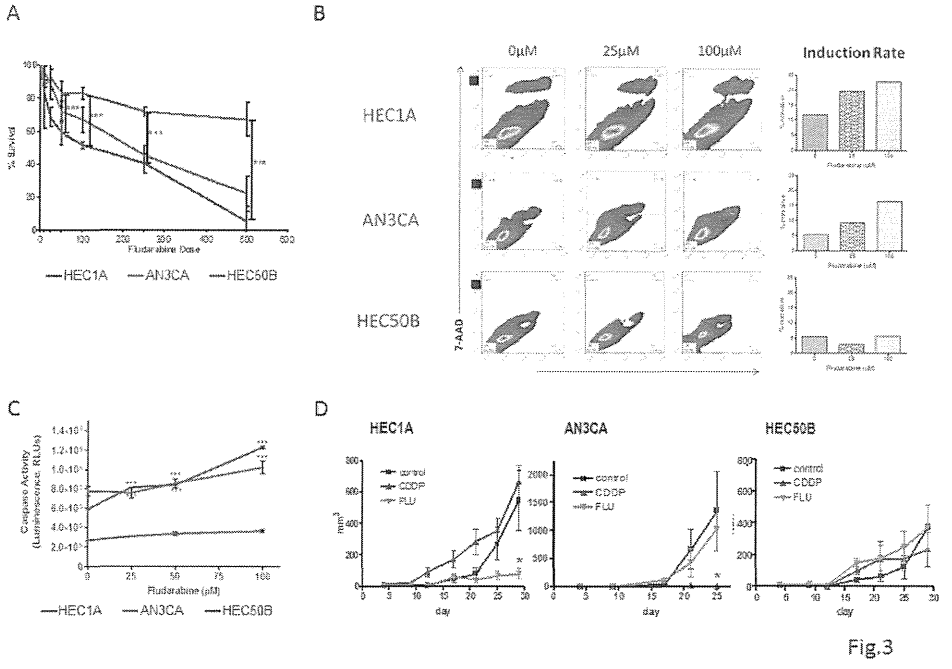

Fig.3

240x173mm (300 x 300 DPI)

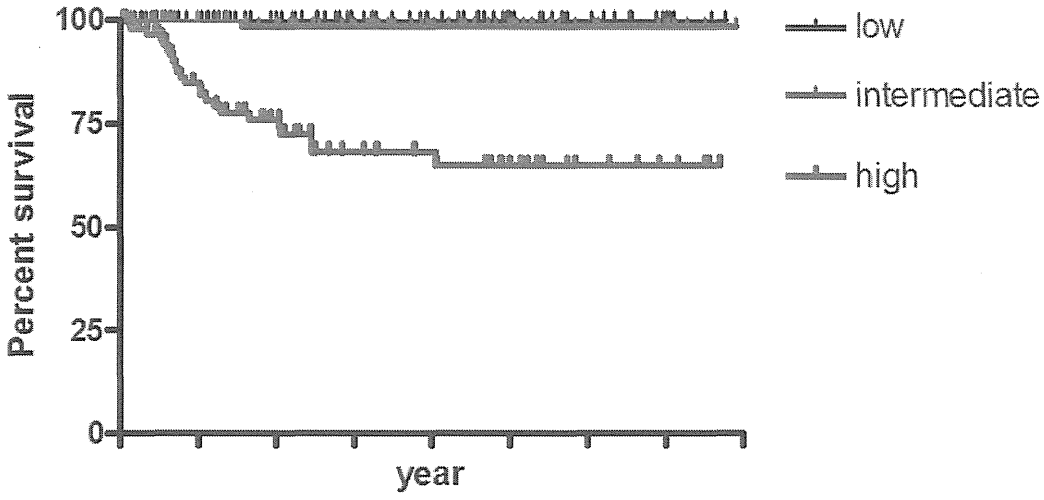

Supplementary Fig.1

A

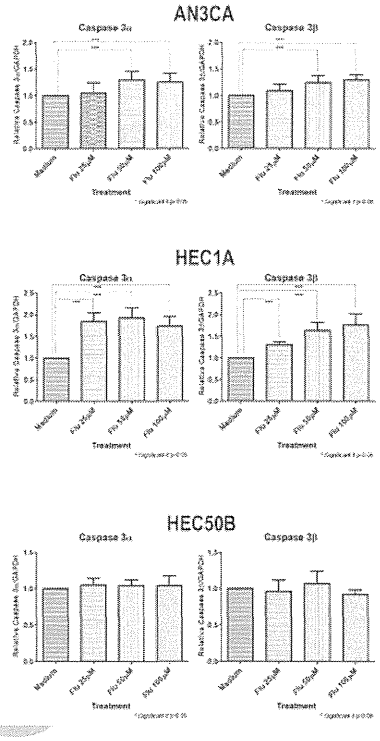

B

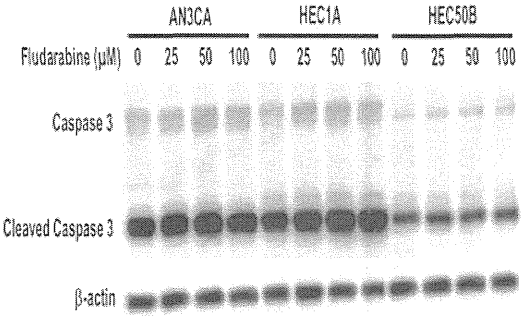

Supplementary Fig.2

Published OnlineFirst January 22, 2013; DOI: 10.1158/1078-0432.CCR-12-2199

Clinical Cancer Research

PD-L1 on Tumor Cells Is Induced in Ascites and Promotes Peritoneal Dissemination of Ovarian Cancer through CTL Dysfunction

Kaoru Abiko, Masaki Mandai, Junzo Hamanishi, et al.

Clin Cancer Res 2013;19:1363-1374. Published OnlineFirst January 22, 2013.

Published OnlineFirst January 22, 2013; DOI: 10.1158/1078-0432.CCR-12-2199

Human Cancer Biology

Clinical Cancer Research

PD-L1 on Tumor Cells Is Induced in Ascites and Promotes Peritoneal Dissemination of Ovarian Cancer through CTL Dysfunction

Kaoru Abiko[1], Masaki Mandai[1], Junzo Hamanishi[1], Yumiko Yoshioka[1], Noriomi Matsumura[1], Tsukasa Baba[1], Ken Yamaguchi[1,2], Ryusuke Murakami[1], Ayaka Yamamoto[1], Budiman Kharma[1], Kenzo Kosaka[1], and Ikuo Konishi[1]

Abstract

Purpose: Ovarian cancer often progresses by disseminating to the peritoneal cavity, but how the tumor cells evade host immunity during this process is poorly understood. Programmed cell death 1 ligand 1 (PD-L1) is known to suppress immune system and to be expressed in cancer cells. The purpose of this study is to elucidate the function of PD-L1 in peritoneal dissemination.

Experimental Design: Ovarian cancer cases were studied by microarray and immunohistochemistry. PD-L1 expression in mouse ovarian cancer cell line in various conditions was assessed by flow cytometry. PD-L1–overexpression cell line and PD-L1–depleted cell line were generated, and cytolysis by CTLs was analyzed, and alterations in CTLs were studied by means of timelapse and microarray. These cell lines were injected intraperitoneally to syngeneic immunocompetent mice.

Results: Microarray and immunohistochemistry in human ovarian cancer revealed significant correlation between PD-L1 expression and peritoneal positive cytology. PD-L1 expression in mouse ovarian cancer cells was induced upon encountering lymphocytes in the course of peritoneal spread *in vivo* and coculture with lymphocytes *in vitro*. Tumor cell lysis by CTLs was attenuated when PD-L1 was overexpressed and promoted when it was silenced. PD-L1 overexpression inhibited gathering and degranulation of CTLs. Gene expression profile of CTLs caused by PD-L1–overexpressing ovarian cancer was associated with CTLs exhaustion. In mouse models, PD-L1 depletion resulted in inhibited tumor growth in the peritoneal cavity and prolonged survival.

Conclusion: PD-L1 expression in tumor cell promotes peritoneal dissemination by repressing CTL function. PD-L1–targeted therapy is a promising strategy for preventing and treating peritoneal dissemination. *Clin Cancer Res; 19(6); 1363–74. ©2012 AACR.*

Introduction

Ovarian cancer is the most lethal disease among gynecologic malignancies. Unlike other epithelial tumors, peritoneal dissemination is the most common mechanism of disease progression in ovarian cancer, and up to 70% of cases present with massive malignant ascites and peritoneal implants (1). Control of dissemination seems to be the most important strategy in controlling ovarian cancer because the median overall survival and progression-free survival are 81.1 and 35.0 months, respectively, if macroscopically complete surgical resection of the disseminated tumors is achieved in Federation Internationale des Gynaecologistes et Obstetristes (FIGO) stage IIIc cancers, whereas these measures are only 34.2 and 14.5 months, respectively, if the disseminated tumor remains after the initial surgery (2). The peritoneal cavity is also the most frequent site of recurrence, and most patients who undergo intraperitoneal recurrence die from this disease (3).

At least 3 steps, cell detachment, immune evasion, and implantation, are required for dissemination. Various molecules expressed by cancer cells have been reported to be involved in these steps (4). In cell detachment, molecules that cause epithelial-to-mesenchymal transition, such as TGF-β or Snail, have an important role (5–7). In implantation, extracellular matrix proteins and VEGF are thought to be important (8). In addition, cancer cells potentially must escape from attack by the immune cells that they encounter in the peritoneal cavity. Immune evasion during peritoneal dissemination is the most enigmatic step. Lymphocytes isolated from malignant ascites have shown

Authors' Affiliations: [1]Department of Gynecology and Obstetrics, Graduate School of Medicine, Kyoto University; and [2]Department of Obstetrics and Gynecology, Japan Baptest Hospital, Kyoto, Japan

Note: Supplementary data for this article are available at Clinical Cancer Research Online (http://clincancerres.aacrjournals.org/).

Corresponding Author: Masaki Mandai, Department of Gynecology and Obstetrics, Graduate School of Medicine, Kyoto University, 54 Shogoin Kawahara-cho, Sakyo-ku, Kyoto 606-8507, Japan. Phone: 81-75-751-3269; Fax: 81-75-761-3967; E-mail: mandai@kuhp.kyoto-u.ac.jp

doi: 10.1158/1078-0432.CCR-12-2199

Published OnlineFirst January 22, 2013; DOI: 10.1158/1078-0432.CCR-12-2199

Translational Relevance

Immune evasion is one of the emerging hallmarks of cancer, though most of its mechanisms remain unveiled. Ovarian cancer often progresses by disseminating to the peritoneum, but how the tumor cells evade host immunity during this process is poorly understood. In this study, we have shown that ovarian cancer cells express programmed cell death 1 ligand 1 (PD-L1) upon encountering lymphocytes in the peritoneal cavity, and as a consequence, inhibit CTL function, escape from CTLs, and disseminate into the peritoneal cavity. Depleting PD-L1 expression in tumor cells resulted in inhibited tumor growth in the peritoneal cavity and prolonged survival of the mice. These data show for the first time that host–tumor immunity, especially tumor immune escape mechanisms, has a pivotal role in peritoneal dissemination. Our data suggest that restoring immune function by inhibiting immune-suppressive factors such as PD-L1 is a promising strategy for controlling the peritoneal dissemination of malignant tumors, including ovarian cancer.

tumoricidal activity (9), but the mechanisms by which the tumor cells evade these cells are not clearly understood. Secretion of Fas ligands by ovarian cancer cells (10), the recruitment of regulatory T cells (11), and the T-cell suppressor cytokine phenotype of monocytes and macrophages (12) have been reported to be included in this step, but the precise mechanism of tumor evasion from immune cells remains unclear.

Recent studies have added immune evasion as one of the important hallmarks of cancer (13). Restoring immune function in cancer microenvironment has immense potential for a new cancer therapy (14). We have attempted to elucidate the mechanism of immune escape in ovarian cancer and reported that in the ovarian cancer microenvironment, molecules such as ULBP2 (NKG2D ligand), COX-1, COX-2, and programmed cell death 1 ligand 1 (PD-L1) or the combined expression of these molecules are related to limited infiltration by lymphocytes and an unfavorable prognosis (15–18). PD-L1 (also known as B7-H1 or CD274) is a coregulatory molecule that is expressed on the surface of various types of cells, including immune cells and epithelial cells. By binding to its receptor PD-1 on lymphocytes, it generates an inhibitory signal toward the T-cell receptor (TCR)-mediated activation of lymphocytes (19, 20). We have reported that PD-L1 expression in tumor cells is an independent unfavorable prognostic factor in human ovarian cancer (15), and that PD-L1 expression showed the closest relation to unfavorable prognosis among other immunosuppressive molecules that we have tested (18). These data suggest that PD-L1 has a role in the clinical course of ovarian cancer by affecting the local immune microenvironment and that PD-L1/PD-1 signal could be a potential therapeutic target. Actually, a recent clinical trial of systemic administration of anti-PD-1 or anti-PD-L1 antibody showed a promising clinical effect in several solid tumors (21–23). However, the role of PD-L1 or the precise mechanism of immune escape in the process of peritoneal dissemination is poorly understood.

The aim of this study was to investigate the mechanism by which PD-L1 on cancer cells in ascites enables immune evasion during peritoneal dissemination, by using both clinical samples and mouse models.

Materials and Methods

Survival analysis of ovarian cancer patients

A total of 65 patients with epithelial ovarian cancer (KOV-IH-65), who underwent primary operation at Kyoto University Hospital (Kyoto, Japan) between 1997 and 2002 and the outcome and peritoneal cytology was evaluable from the chart was included in the study under the approval of the Kyoto University Graduate School and Faculty of Medicine Ethics Committee. Ascites or the peritoneal wash fluid was collected at operation and served for pathologic diagnosis. Patient characteristics are listed in Supplementary Table S1.

Microarray profiling of ovarian cancer tissues

Ovarian cancer specimens were obtained from 64 patients (KOV-MA-64), who underwent primary surgery for epithelial ovarian cancer at Kyoto University Hospital between 1997 and 2011. Ten patients in KOV-IH-65 were included in KOV-MA-64. All tissue specimens were collected under written consent approved by the Facility Ethical Committee. Patient characteristics are listed in Supplementary Table S1. Samples were selected to have more than 70% tumor cell nuclei and less than 20% necrosis. Total RNA expression was analyzed on Human Genome U133 Plus 2.0 Array (Affymetrix). Robust multiarray average (RMA) normalization was conducted using R (R: a language and environment for statistical computing; http://www.R-project.org.). Probes showing expression value more than 5.0 in at least one of the samples and SD more than 0.2 across all the samples were selected, and *t* test was conducted between cytology-positive and -negative groups. Enrichment for Gene Ontology terms was analyzed using GOEAST software (http://omicslab.genetics.ac.cn/GOEAST/; ref. 24) for the set of probes highly expressed in cytology-positive or -negative groups, respectively ($P < 0.05$). A publicly accessible gene set of IFN-γ–upregulated genes was downloaded (http://www.broadinstitute.org/gsea/msigdb/geneset_page.jsp?geneSetName=SANA_RESPONSE_TO_IFNG_UP; ref. 25). Gene set enrichment analysis (GSEA) for positive ascites cytology and negative cytology was conducted using GSEA software (http://www.broadinstitute.org/gsea/downloads.jsp).

Immunohistochemistry

Formalin-fixed, paraffin-embedded specimens of ovarian cancer were obtained from KOV-IH-65 patients under written consent as earlier. Immunohistochemical staining for PD-L1 was conducted using a PD-L1 antibody as previously described (15, 18). PD-L1 expression was analyzed by 2

Published OnlineFirst January 22, 2013; DOI: 10.1158/1078-0432.CCR-12-2199

independent gynecologic pathologists without any prior information about the clinical history of the patients, and the samples were categorized into a positive expression group (equal to or stronger than the positive control) and a negative expression group (weaker than the positive control) based on the intensity of the staining. Placenta was used as positive control. Samples with staining in less than 50% of tumor cells was considered negative.

Animals

Female C57BL/6 (B6) and B6C3F1 and C.B-17/Icr-scid/scidJcl [severe combined immunodeficient mice (SCID)] mice were purchased from CLEA Japan. OT-1 mice and CAG-GFP mice were purchased from the Jackson Laboratory and were interbred to generate OT-1-GFP mice. Animal experiments were approved by the Kyoto University Animal Research Committee, and animals were maintained under specific pathogen-free conditions. To evaluate the effect of PD-L1 on the survival and progression of peritoneal dissemination and ascites formation, HM-1 cells (1×10^6) or ID8 cells (5×10^6) were injected into the abdominal cavity. The body weight gain was calculated every other day. Mice were euthanized before reaching the moribund state.

Cell lines

The ID8 mouse ovarian cancer cell line (26, 27) was kindly provided by Dr. Margit Maria Janát-Amsbury (Department of Obstetrics and Gynecology, Division of Gynecologic Oncology, Baylor College of Medicine, Houston, TX; ref 27). The cells were maintained in RPMI-1640 medium (Nacalai Tesque) supplemented with 10% FBS (v/v; Biowest) and penicillin–streptomycin (Nacalai Tesque). The OV2944-HM-1 (HM-1) mouse ovarian cancer cell line was purchased from RIKEN BioResource Center and cultured as previously described (7). Human ovarian cancer cell lines were cultured as described previously (28). The ID8-GFP cells and HM1-GFP cells were generated by retroviral transfection as described previously (29).

The PD-L1–overexpressing cell lines, ID8-pdl1 and HM1-pdl1, were generated by lentiviral transfection of ViraPower pLenti6/V5-DEST Gateway Vector (Invitrogen) carrying mouse PD-L1 cDNA. Full-sequenced cDNA was purchased from OpenBiosystems and amplified by PCR using the following primers:

Forward; CACCAACATGAGGATATTTGCTGG
Reverse; TCAACACTGCTTACGTCTCC

Expression vector was generated using pENTR Directional TOPO Cloning Kit (Invitrogen).

The PD-L1–depleted cell lines, ID8-Mirpdl1 and HM1-Mirpdl1, were generated using the BLOCK-iT HiPerform Lentiviral Pol II miR RNAi Expression System with EmGFP (Invitrogen) according to the protocol provided by the manufacturer. Briefly, double-stranded oligos were generated from designed single-stranded DNA oligos listed later, and cloned into pcDNA™6.2-GW/EmGP-miR expression vector. Then, it was linearized and BP/LR Reaction was conducted using pDONR™221 vector and pLenti6.4/R4R2/V5-DEST and pENTR™5′ promoter clone to generate Lentiviral expression clone. The sequence of the miR DNA oligos used for PD-L1 depletion is as follows:

Top strand oligo;
TGCTGTTCAACGCCACATTTCTCCACGTTTTGGCCACTGACTGACGTGGAGAAGTGGCGTTGAA
Bottom strand oligo;
CCTGTTCAACGCCACTTCTCCACGTCAGTCAGTGGCCAAAACGTGGAGAAATGTGGCGTTGAAC

Sequence control cell lines (ID8-control and HM1-control) were generated using a nonsilencing miR oligo provided by the manufacturer.

A concentration of 20 ng/mL recombinant human IFN-γ (R&D Systems) or recombinant mouse IFN-γ (PeproTech) was added to the culture medium for 24 hours before analysis for IFN-γ stimulation. For the other recombinant mouse cytokines, 200 ng/mL interleukin (IL)-2 (eBioscience) or 20 ng/mL IL-6 (R&D Systems), TGF-β (PeproTech), IL-10 (PeproTech), or TNF-α (PeproTech) was added to the culture medium for 24 hours before analysis.

Flow cytometry

Cultured cells were harvested and incubated with phycoerythrin (PE)-conjugated PD-L1 (mouse clone MIH5, human clone MIH1; BD Biosciences) or a matched isotype control (BD Biosciences) at 4°C for 30 minutes, washed twice, and analyzed using a FACSCalibur cytometer (Beckton Dickinson). The results were analyzed using CellQuest Pro software.

Analysis of PD-L1 expression on tumor cells in ascites

Mice were challenged with an intraperitoneal injection of the GFP-labeled cell lines. Mice with ascites formations were sacrificed and the ascites were collected. After briefly centrifuging, red blood cells were lysed, and the remaining cells were washed twice, incubated with antibodies, and analyzed by flow cytometry as mentioned previously. 7-AAD Staining Solution (BD Biosciences) was added 10 minutes before analysis to gate out nonviable cells. GFP-positive and 7-amino-actinomycin D–negative gated cells were analyzed as ascites tumor cells.

$CD8^+$ T lymphocyte collection from ascites

Mouse ascites cells were collected and washed with PBS supplemented with 2% FBS. $CD8^+$ T lymphocyte was collected by magnetic separation using mouse CD8a MicroBeads (Miltenyi Biotec).

Detection of intracellular IFN-γ in mouse lymphocytes

For intracellular IFN-γ staining, BD Cytofix/Cytoperm Fixation/Permeabilization Kit (BD Biosciences) and PE-conjugated anti-mouse IFN-γ antibody (BD Biosciences) were used. A matched isotype control was used to determine IFN-γ–negative quadrant. PerCP-conjugated anti-mouse CD3e antibody (BD Biosciences), Alexa Fluor 647-

Published OnlineFirst January 22, 2013; DOI: 10.1158/1078-0432.CCR-12-2199

conjugated anti-mouse CD8a antibody (BD Biosciences), and fluorescein isothiocyanate (FITC)-conjugated anti-mouse CD4 antibody were used to gate lymphocytes and $CD4^+$ or $CD8^+$ cells.

Multiplexed bead assay for cytokines in ascites

BD CBA Mouse Th1/Th2/Th17 Kits (BD Biosciences) was used according to the manufacturer's protocol. Concentrations of each cytokines were calculated using BD Cytometric Bead Array Software version 1.4 (BD Biosciences).

Proliferation assay

A water soluble tetrazolium–8 assay using Cell Count Reagent SF (Nacalai Tesque) was conducted according to the manufacturer's protocol, and the proliferation rate for each cell line was calculated and plotted.

Activation of CTLs

B6 splenocytes underwent T-cell depletion using CD90.2 Microbeads (Miltenyi Biotec) and were incubated with 10 μg/mL $OVA_{257-264}$ peptide (SIINFEKL, Bachem Bioscience) at 37°C for 1 hour. Then they were coincubated with $CD8^+$ cells that were isolated from female OT-1-GFP mice using $CD8a^+$ T Cell Isolation Kit II (Miltenyi Biotec) for 4 to 6 days. Subsequently, the CTLs were collected by CD8a MicroBeads (Miltenyi Biotec) and were used for further experiments. RPMI-1640 medium supplemented with 10% FBS, 50 μmol/L 2-mercaptoethanol (Nacalai Tesque), 2 mmol/L L-glutamine (Invitrogen), and penicillin–streptomycin (Nacalai Tesque) was used for lymphocyte cultures.

Cytotoxicity assay

As target cells, ID8 cells were loaded with 10 μg/mL $OVA_{257-264}$ peptide (Bachem Bioscience) at 37°C for 1 hour. As effectors, activated OT-1 $CD8^+$ CTLs were prepared as described earlier. The target cells were cocultured with the effector cells at various E/T (effector-to-target) ratios. After 5 hours of incubation, the levels of lactate dehydrogenase in the culture supernatant were determined using the cytotoxicity detection kit CytoTox96 (Promega). We used 0.9% Triton X to determine maximum target cell lysis. Percentage lysis was calculated according to a modified standard formula:

$$(OD_{experimental} - OD_{spontaneous\ targets} - OD_{spontaneous\ effectors})/(OD_{maximum} - OD_{spontaneous\ targets}) \times 100.$$

CD107a expression assay

After 4 hours of coincubation of target cells and OT-1-GFP mouse CTLs at an E/T ratio of 30, the cells were incubated with an Alexa Fluor 647–conjugated anti-CD107a antibody (BioLegend) and were washed twice and analyzed by flow cytometry. GFP-positive cells were gated as OT-1-GFP mouse CTLs.

Time-lapse photography of CTLs attacking target cells

CTLs from OT-1-GFP mouse were activated as described earlier. A total of 3×10^6/mL CTLs were mixed with 1×10^5/mL ID8-control or ID8-pdl1 cells loaded with OVA peptide and observed under a laser microscope (Olympus TH4-100) at magnification of ×200. Images of GFP-positive cells were acquired every 2 minutes for total of 68 times (=136 minutes) using DP71-MetaMorph system. Time-lapse video was made from these images (10 frames/s) using MetaMorph software (Molecular Devices).

Microarray profiling of CTLs

OT-1-GFP-mouse CTLs were collected from 4 mice (mouse A to D) and activated as described earlier. CTLs from mouse A to D were divided into 2 groups and coincubated with ID8-pdl1 (PD-L1 group) or ID8-Mirpdl1 (Mir group) for 4 hours at an E/T ratio of 30. Then, the activated CTLs were collected by magnetic separation using CD8a Microbeads (Miltenyi Biotec). From these 8 samples of CTLs, whole RNA was extracted with RNAeasy Kit (Qiagen) and hybridized to Affymetrix Mouse Genome430 2.0 Array as previously described (5). RMA normalization was conducted as described earlier. Gene sets for CTL_PD-L1_UP (high in PD-L1 group) and CTL_PD-L1_DN (high in Mir group) were generated using paired t test between the 2 groups ($P < 0.01$). GSE24026 dataset, which analyzed downstream of PD-1 signaling (30), was downloaded from Gene Expression Omnibus (GEO) DataSets (http://www.ncbi.nlm.nih.gov/gds) to analyze the association of PD-1 signaling with our experiments.

Statistics

For the analysis of immunohistochemistry, Fisher exact test and the χ^2 test were used to analyze the associations between PD-L1 expression and ascites cytology. Survival was analyzed using the Kaplan–Meier survival analysis with the log-rank test by GraphPad Prism 5 software. A P value less than 0.05 was considered to be significant.

Results

Positive cytology of peritoneal wash or ascites is related to poor overall and progression-free survival in ovarian cancer patients

Survivals of 65 patients with ovarian cancer (KOV-IH-65) were studied. A cytologic examination at the time of operation revealed viable malignant cells in the ascites of 42 patients ("cytology-positive" cases) in this group. Positive cytology was related to poor overall survival ($P < 0.001$; Supplementary Fig. S1A) and poor progression-free survival ($P < 0.001$; Supplementary Fig. S1B) indicating that positive cytology in ascites was a significant poor prognostic factor in ovarian cancer as previously reported (1, 4).

Genes in Gene Ontology term related to immunity are enriched in cytology-positive cases

Microarray analysis of ovarian cancer tissue from 64 patients (KOV-MA-64) was conducted. Thirty patients were cytology positive in this group. Among 1,692 probes that were highly expressed in ascites-cytology–positive cases,

Published OnlineFirst January 22, 2013; DOI: 10.1158/1078-0432.CCR-12-2199

genes belonging to Gene Ontology terms related to immunity, such as "regulation of immune system process," "positive regulation of immune effector process," or "regulation of IFN-γ production" were enriched. Significantly enriched Gene Ontology terms in cytology-positive cases are listed in Supplementary Table S2. PD-L1 (CD274) was included in Gene Ontology term "regulation of immune system process."

Genes upregulated by IFN-γ, including PD-L1, are enriched in cytology-positive cases

GSEA revealed that the genes upregulated in response to IFN-γ were significantly enriched in cytology-positive cases in KOV-MA-64 (Fig. 1A). FDR q value was 0.242. Genes upregulated in response to IFN-γ are shown in heatmap in Supplementary Fig. S2. Again, PD-L1 (CD274) was included in the enriched genes. These data indicate that ascites-cytology–positive cases in ovarian cancer are distinctly characterized by regulation of immune response, especially by IFN-γ-induced genes, including PD-L1.

PD-L1 protein expression in human ovarian cancer is related to positive peritoneal cytology and poor prognosis

To determine if PD-L1 protein expression also correlates to the positive peritoneal cytology, immunohistochemistry for PD-L1 in the sampled tissue was conducted (Fig. 1B). Forty-four cases were positive for PD-L1. Positive cytology cases showed tendency to have positive PD-L1 expression in the tumor tissue ($P = 0.048$, χ^2 test; $P = 0.058$, Fisher exact test; Fig. 1C).

Overall survival of PD-L1–positive patients in KOV-IH-65 was significantly shorter ($P = 0.023$) as compared with PD-L1–negative patients (Fig. 1D).

Human and mouse ovarian cancer cell lines express various levels of PD-L1

We examined the PD-L1 expression on several human and mouse ovarian cancer cell lines by flow cytometry. Two of 6 tested human cell lines expressed high levels of PD-L1, whereas 4 cell lines expressed very low levels of or no PD-L1 (Fig. 2A). The mouse ovarian cancer cell line ID8 did not express PD-L1, whereas HM-1 expressed very low level of PD-L1 (Fig. 2B).

Next, we assessed whether IFN-γ alters PD-L1 expression on these cell lines because IFN-γ is reported to induce PD-L1 expression (31, 32). Human recombinant IFN-γ (20 ng/mL) for human cells or mouse recombinant IFN-γ (20 ng/mL) for mouse cells was added to the culture medium. IFN-γ induced PD-L1 expression in 3 human cell lines and in ID8 and HM-1, whereas OV90 did not express PD-L1 even after

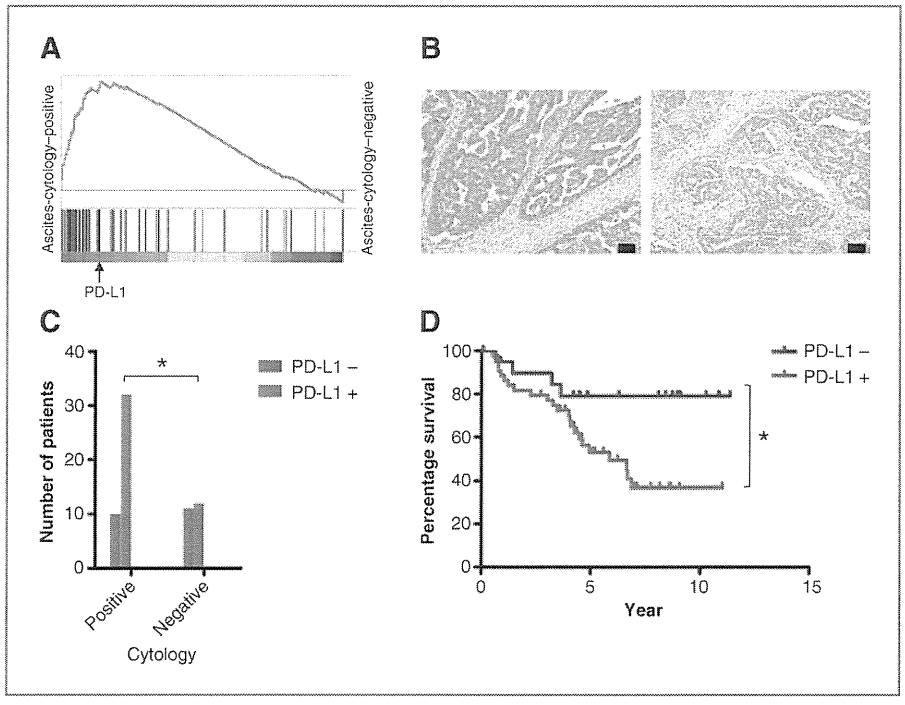

Figure 1. PD-L1 expression on human ovarian cancer cells is related to tumor survival in ascites. A, enrichment of the gene set described for response to IFN-γ in the ascites-cytology–positive cases, relative to the ascites-cytology–negative cases. Black vertical bars represent genes in this gene set. The position of the gene PD-L1 is shown by an arrow. Position to the left indicates enrichment in ascites-cytology–positive cases; a position to the right indicates enrichment in ascites-cytology–negative cases. B, PD-L1 expression in human ovarian cancer tissue. Representative samples with high expression (left) and low expression (right; magnification ×200). Bars, 50 μm. C, the result of immunohistochemistry of PD-L1 in KOV-IH-65. Positive cytology cases tend to have positive PD-L1 expression. *, $P = 0.048$, χ^2 test; $P = 0.058$, Fisher exact test. D, overall survival of KOV-IH-65. PD-L1 immunohistochemistry positive (red line) and negative (blue line). *, $P = 0.023$.

Published OnlineFirst January 22, 2013; DOI: 10.1158/1078-0432.CCR-12-2199

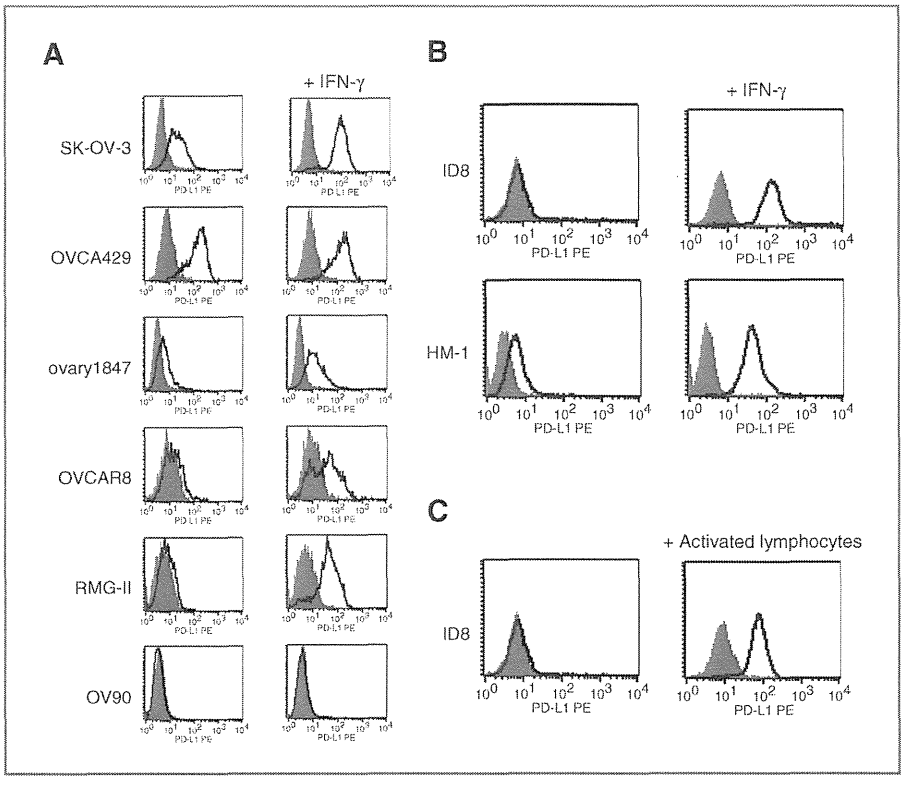

Figure 2. Human and mouse ovarian cancer cell lines express various levels of PD-L1. A, PD-L1 expression in 6 human ovarian cancer cell lines with (right) or without (left) IFN-γ exposure. Shaded histogram, isotype control; open histogram, anti-PD-L1-antibody. B, PD-L1 expression in 2 mouse ovarian cancer cell lines with or without IFN-γ exposure. Shaded histogram, isotype control; open histogram, anti-PD-L1-antibody. C, PD-L1 expression in ID8 cells coincubated with or without activated lymphocytes for 24 hours. Shaded histogram, isotype control; open histogram, anti-PD-L1-antibody.

IFN-γ exposure, indicating that this cell line has some functional loss in IFN-γ pathway (Fig. 2A and B).

Coculture with activated lymphocytes induces PD-L1 expression in mouse ovarian cancer cell lines

To determine whether activated lymphocytes, which are a possible source of IFN-γ *in vivo*, induce PD-L1 on ovarian cancer cells, we cocultured activated lymphocytes with ID8 cells. Lymphocytes from B6 mouse spleen were stimulated with 1 μg/mL of anti-mouse CD3 antibody (BioLegend) and 2 μg/mL of anti-mouse CD28 antibody (BioLegend) for 4 days before the experiment. After 24 hours of coculture, the ID8 cells were analyzed for PD-L1 expression by flow cytometry. PD-L1 expression was markedly increased after coculture with activated lymphocytes (Fig. 2C). Similarly, PD-L1 on HM-1 was also induced by coculture with syngeneic activated lymphocytes (data not shown). Thus, coculture with activated T lymphocytes induces PD-L1 in mouse ovarian cancer cells.

Ovarian cancer cells in mouse ascites express PD-L1 by encountering lymphocytes

As mouse models of ovarian cancer dissemination, ID8 and HM-1 formed cancerous ascites and massive peritoneal dissemination after intraperitoneal injection into syngeneic mice. ID8-GFP cells and HM-1-GFP cells in the ascites expressed PD-L1 (Fig. 3A), and as high as 19% of the $CD8^+$ T lymphocytes in the ascites was positive for intracellular IFN-γ (Fig. 3B). In contrast, IFN-γ concentration in ascites supernatant was very low, whereas IL-6, -10, and TNF-α were detected in higher concentrations (Fig. 3C). We tested IL-2, -6, TGF-β, TNF-α, and IL-10 to determine whether cytokines other than IFN-γ affect PD-L1 expression in the ascites, but none of the tested cytokines induced PD-L1 on HM-1 cells (Fig. 3D). As expected, adding the ascites supernatant to the culture medium did not affect PD-L1 expression on ID8 or HM-1 cells (Fig. 4A). Floating cultures in a nonadherent dish, a hypoxic culture in 1% oxygen, or both, which is a mimic of ascites condition, did not alter PD-L1 expression in HM-1 cells (Fig. 4B). However, coculture with mice ascites cells enhanced PD-L1 expression in HM-1 cells, and coculture with $CD8^+$ cells isolated from mouse ascites induced even higher levels of PD-L1 in HM-1 cells (Fig. 4C).

Administration of HM-1-GFP to a SCID mouse also forms cancerous peritonitis. However, HM-1-GFP cells in SCID mouse ascites did not express PD-L1 (Fig. 4D). These data suggest that the tumor cells express PD-L1 in ascites as a consequence of their encounter with activated lymphocytes.

Generation of PD-L1–overexpressing and PD-L1–depleted cell lines

To examine the effects of PD-L1 expression on tumor cells, we established PD-L1–overexpressing cell lines (denoted ID8-pdl1 and HM1-pdl1) and PD-L1–depleted cell lines (denoted ID8-Mirpdl1 and HM1-Mirpdl1) from the ID8 and HM-1. PD-L1 expression is shown in Supplementary Fig. S1C. To confirm that PD-L1 depletion was successfully

Published OnlineFirst January 22, 2013; DOI: 10.1158/1078-0432.CCR-12-2199

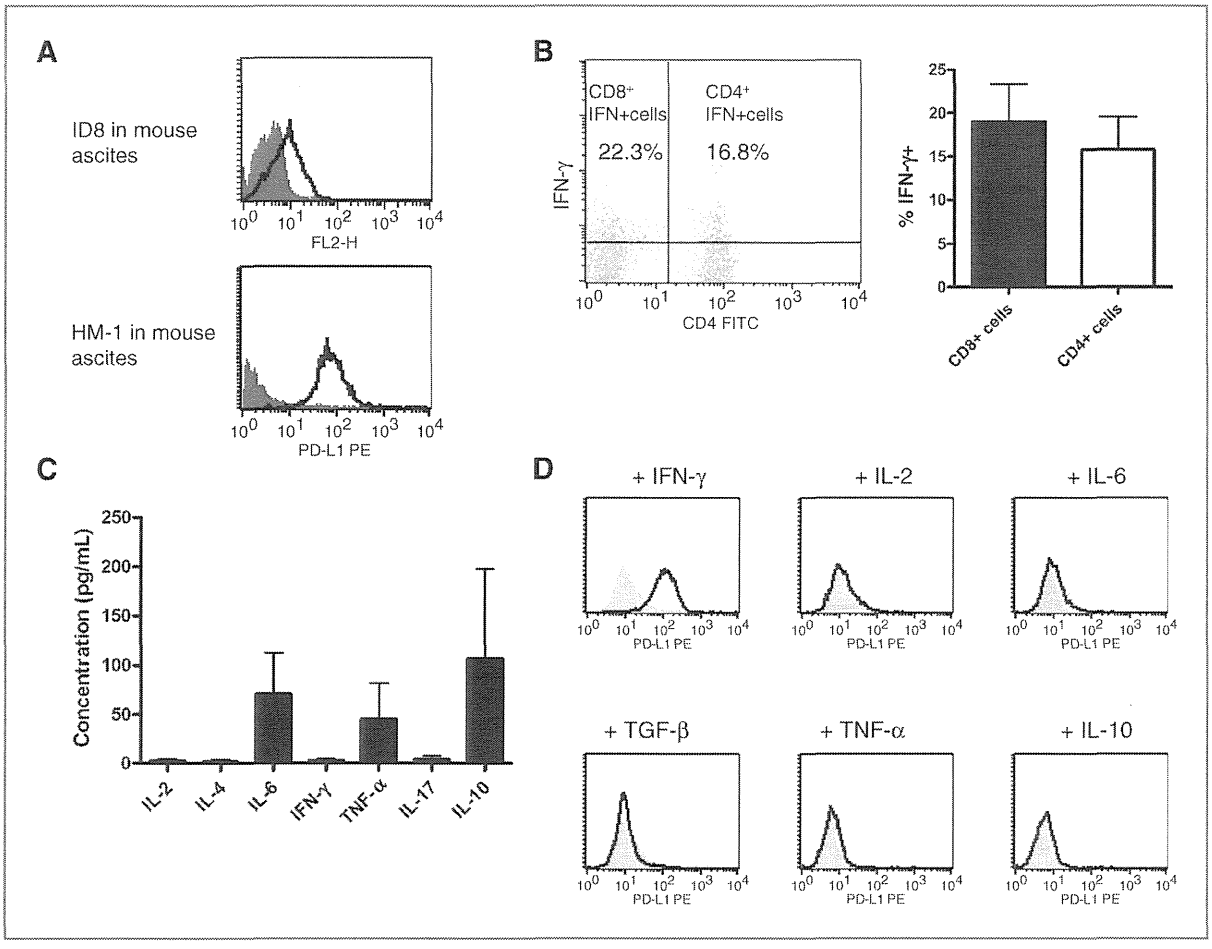

Figure 3. Ovarian cancer cells in mouse ascites express PD-L1. A, ovarian cancer cells in the ascites of the mouse ovarian cancer models express PD-L1. Flow cytometry histograms of ascites cells from a mouse inoculated with ID8-GFP (top) and HM-1-GFP (bottom) are shown. GFP-positive and 7-amino-actinomycin D–negative cells are gated as tumor cells. Shaded histogram, isotype control; open histogram, anti-PD-L1-antibody. Representative of 3 experiments with similar results. B, lymphocytes in the ascites of mouse ovarian cancer model are positive for intracellular IFN-γ. A representative result of 3 experiments (left) and percentage of intracellular IFN-γ–positive cells in mouse ascites T lymphocytes (right). Mean ± SD ($n = 3$). CD3-positive cells are gated. C, cytokine concentration in ID8-bearing mouse ascites supernatant. Mean ± SD ($n = 3$). D, PD-L1 expression after exposure to various cytokines. None of the tested cytokines other than IFN-γ induced PD-L1 on HM-1. Shaded histogram, PD-L1 expression without cytokine; open histogram, PD-L1 expression with cytokine added to the medium 24 hours before the assessment.

achieved, PD-L1–depleted cell line or control cell line was coincubated with ascites cells or ascites $CD8^+$ cells, and PD-L1 expression in the depleted cell line was lower than in the control cell lines (Supplementary Fig. S1D).

In vitro cell proliferation is not affected by PD-L1 expression

A cell proliferation assay revealed that the proliferation curves of the PD-L1–manipulated cell lines were similar to those of the control cell lines (Fig. 5A), indicating that PD-L1 expression does not affect cell proliferation *in vitro*.

PD-L1 protects ovarian cancer cells from antigen-specific cytolysis by CTLs

We next conducted a cytotoxicity assay to examine antigen-specific cytolysis by $CD8^+$ CTLs. The cytotoxicity curves were significantly different between the cell lines. High levels of target cell lysis were observed in ID8-Mirpdl1 cells, and low levels of target cell lysis were observed in ID8-pdl1 cells (Fig. 5B), indicating that antigen-specific cytolysis by CTLs is inhibited by PD-L1 and can be promoted by PD-L1 depletion.

CTL function is inhibited by tumor-associated PD-L1

Alterations in CTLs following their encounter with tumor-associated PD-L1 were assessed. CTLs lyse target cells by secreting perforin and granzymes, and CD107a is a surface marker for the degranulation of activated CTLs. CD107a expression in the CTLs cocultured with ID8-pdl1 was weaker than control, indicating that T-cell degranulation following antigen stimulation has been inhibited by tumor-associated PD-L1 (Fig. 5C). Under microscopic

Published OnlineFirst January 22, 2013; DOI: 10.1158/1078-0432.CCR-12-2199

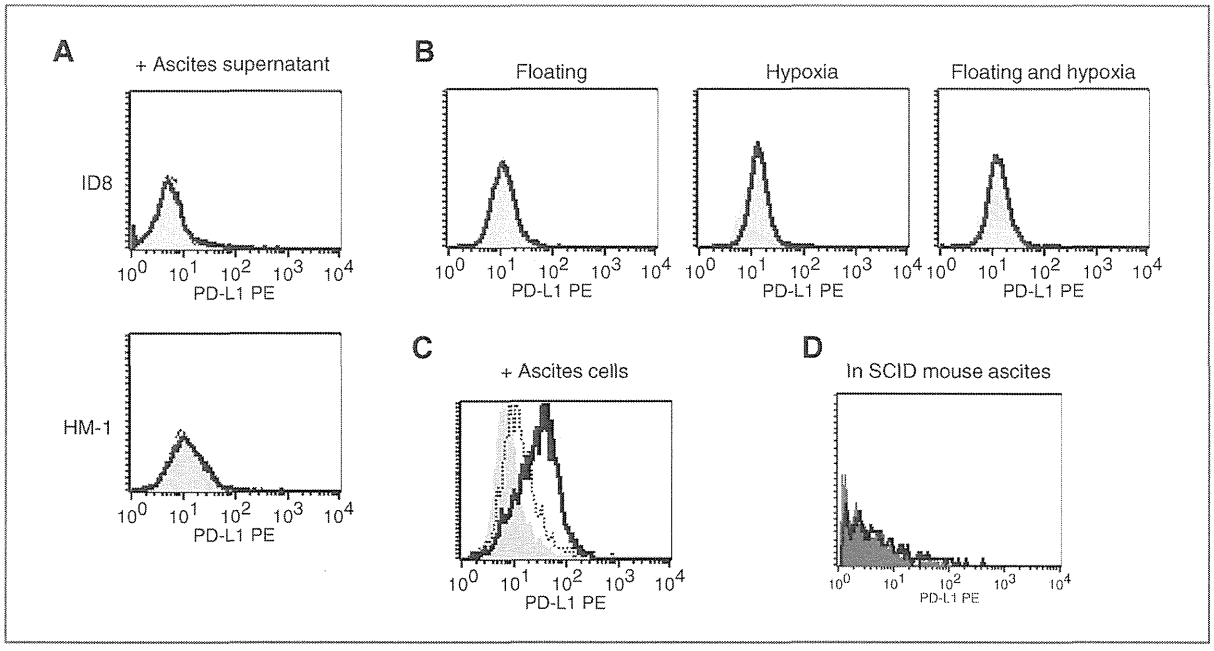

Figure 4. Lymphocytes in ascites induce PD-L1 on mouse ovarian cancer cells. A, ascites supernatant did not induce PD-L1 in ID8 or HM-1 cells. Shaded histogram, isotype control; open histogram, anti-PD-L1 antibody. Representative of 3 repeated independent experiments with similar results. B, PD-L1 expression under various culture conditions. Floating culture in nonadherent dish, culture under hypoxic condition (1% O_2), or both did not affect PD-L1 expression. Shaded histogram, PD-L1 expression in normal culture condition; open histogram, PD-L1 expression under floating, hyoxic, or both floating and hypoxic conditions. Representative of 3 repeated independent experiments with similar results. C, $CD8^+$ T cells from mouse ascites induce PD-L1 expression on HM-1. Shaded histogram, cultured without any ascites cells; dotted line histogram, ascites cells added to the culture; solid line histogram, ascites $CD8^+$ cells added to the culture. Representative of 3 repeated independent experiments with similar results. D, mouse ovarian cancer cells in SCID mouse ascites do not express PD-L1. Representative of 3 mice with similar results.

observation while coculturing with these target cells, CTLs gathering to the tumor cells were markedly inhibited in ID8-pdl1 (Fig. 5D and Supplementary Videos S1 and S2). These results indicate that PD-L1 on tumor cells inhibit CTL function.

Gene expression profile of mouse CTLs affected by PD-L1 shows correlations to PD-1 signal genes in human

PD-L1 is reported to transmit an inhibitory signal through its receptor, PD-1, in lymphocytes. To examine the alteration in gene expression profiles in mouse CTLs associated with PD-L1, microarray analysis for CTLs coincubated with ID8-pdl1 or ID8-Mirpdl1 was conducted, and the gene expression profile was compared by GSEA with a publicly accessible gene set of human functionally impaired $CD8^+$ T cells by positive PD-1 signal (30). Up- and downregulated genes in mouse CTLs are shown in Supplementary Table S3. Interestingly, the genes upregulated in PD-L1–affected mouse CTLs were significantly enriched in upregulated genes in PD-1 downstream genes in human CTLs. Furthermore, the genes downregulated in PD-L1–affected mouse CTLs were also significantly downregulated in PD-1 signal-transmitted human CTLs (Supplementary Table S4). This result is consistent with the fact that PD-L1 on tumor cells transfers inhibitory signal through PD-1 on CTLs and also validate the similar mechanism of PD-L1/PD-1 effect in human and mouse CTLs.

PD-L1 promotes tumor progression in mouse ovarian cancer dissemination models

HM-1-pdl1, HM-1-Mirpdl1, or HM1-control cells were injected intraperitoneally to syngeneic mice. After 7 days, the body weight of the mice, a reliable marker of tumor growth, in all 3 groups increased (Fig. 6A). However, in the HM1-Mirpdl1 group, the body weight decreased after 10 days (Fig. 6A, right). Therefore, PD-L1 depletion decreased the tumor that once grew in the peritoneal cavity.

The survival of the mice is shown in Fig. 6B–D. The HM-1-pdl1 group lived shorter ($P = 0.039$) than the control group, and the HM-1-Mirpdl1 group lived longer ($P = 0.0029$; Fig. 6B). In ID8-injected mice, the survival of the ID8-pdl1 group and the ID8-control group were similar (Fig. 6C), indicating that differences in PD-L1 expression upon injection is eventually abrogated in slow-progressing tumors because PD-L1 is induced in the peritoneal cavity. However, the mice in the ID8-Mirpdl1 group had significantly longer survival times than the control group ($P < 0.001$; Fig. 6C). PD-L1 expression in tumor cells did not affect the survival of SCID mice following intraperitoneal injection (Fig. 6D).

Discussion

Although various molecules expressed by cancer cells have been implicated in the process of peritoneal dissemination, the influence of immunologic factors is poorly understood. In this study, we first focused on the state of

Published OnlineFirst January 22, 2013; DOI: 10.1158/1078-0432.CCR-12-2199

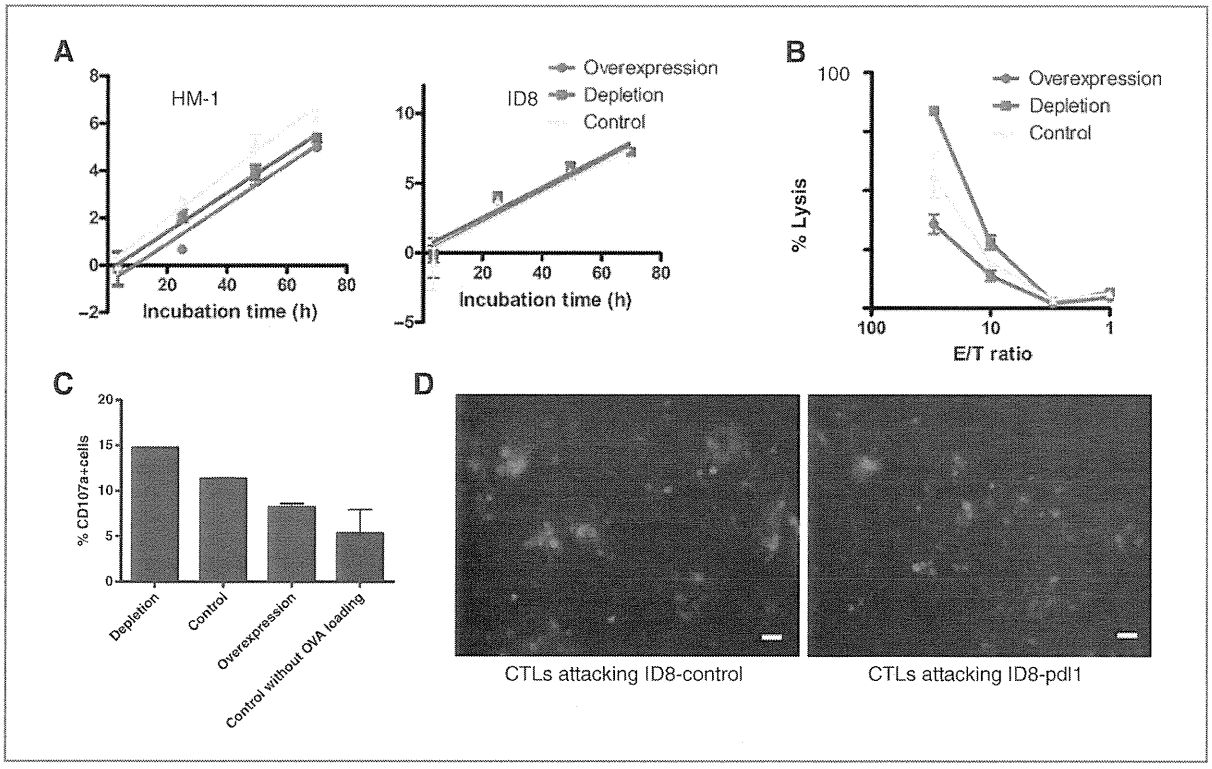

Figure 5. PD-L1 protects tumor cells from CTLs. A, cell proliferation assay of the PD-L1–manipulated HM-1 cell lines (left) and ID8 cell lines (right). *Y*-axis, relative number of cells in $\log_2$ scale. *X*-axis, incubation time (h). Mean ± SD ($n = 6$) from 1 representative experiment of 2 repeated experiments with similar results. Relative number of cells is calculated in the following formula: (Relative number of cells) = (number of cells estimated by water soluble tetrazolium–8 assay)/(seeded cells). B, cytotoxicity assay of the PD-L1–manipulated ID8 cell lines. Mean ± SD ($n = 4$) from 1 representative experiment of 3 repeated experiments with similar results. C, $CD107a^+$ CTLs following coincubation with OVA-loaded ID8-Mirpdl1, OVA-loaded ID8-control, OVA-loaded ID8-pdl1, or ID8-control without OVA loading. Mean ± SD ($n = 3$) from 1 of 3 repeated experiments with similar results. D, microscopic image of activated GFP+ CTLs, after 136 minutes of coincubation with ID8-control (left) or ID8-pdl1 (right). Bars, 50 μm. Time-lapse video available in Supplementary Videos S1 and S2. One of 3 repeated experiments with similar results.

"positive peritoneal cytology," which represents the status that the tumor cells are surviving in peritoneal cavity without being destroyed by host immunity. We confirmed that positive cytology adversely affects the overall and progression-free survival of the patients. Then, we analyzed PD-L1 expression in the primary tumor, both in mRNA and protein levels, and found for the first time that it significantly correlates to positive peritoneal cytology. Furthermore, in microarray analyses, gene profile associated with positive peritoneal cytology was significantly enriched of immune-related genes, including PD-L1, assessed by a Gene Ontology analysis. An IFN-γ–induced gene signature, which also includes PD-L1, was also significantly associated with positive peritoneal cytology by GSEA. Together, these data imply that peritoneal spread of ovarian cancer accompanies with local immune modification, and that PD-L1 functions as a key molecule in this process. These data prompted us to further investigate the function of PD-L1 in ovarian cancer cells, especially as related to the peritoneal dissemination.

The mechanism by which PD-L1 expression is regulated is quite ambiguous, especially in cancer cells. In an early report, PD-L1 was reported to be expressed only in immune cells under natural circumstances and to be highly expressed in some tumor cells (31). Subsequent reports have shown that PD-L1 is expressed constitutively in some normal tissues including eyes and placenta (33, 34), and that PD-L1 can be induced in cancer cells and noncancer cells by IFN-γ (35, 36). However, the precise mechanism of PD-L1 induction, especially *in vivo*, is still unclear. Therefore, we initially examined PD-L1 expression under natural culture conditions as well as upon various cytokine stimulations, including IFN-γ, in 6 human and 2 mouse ovarian cancer cell lines. The results suggest that there are 3 types of cells with regards to PD-L1 expression: type A cells (e.g., SK-OV-3) always express PD-L1; type C cells (e.g., OV90) never express PD-L1; and type B cells (e.g., OVARY1847) do not express PD-L1 at baseline but express PD-L1 when exposed to IFN-γ. Type B was most frequent in the tested human ovarian cancer cell lines. It is assumed that PD-L1 expression is not constitutive in these cells but is induced by the influence of other factors. In a mouse experiment, we used 2 type B mouse ovarian cancer cells, ID8 and HM-1. Both cell lines expressed PD-L1 when administered into the

Published OnlineFirst January 22, 2013; DOI: 10.1158/1078-0432.CCR-12-2199

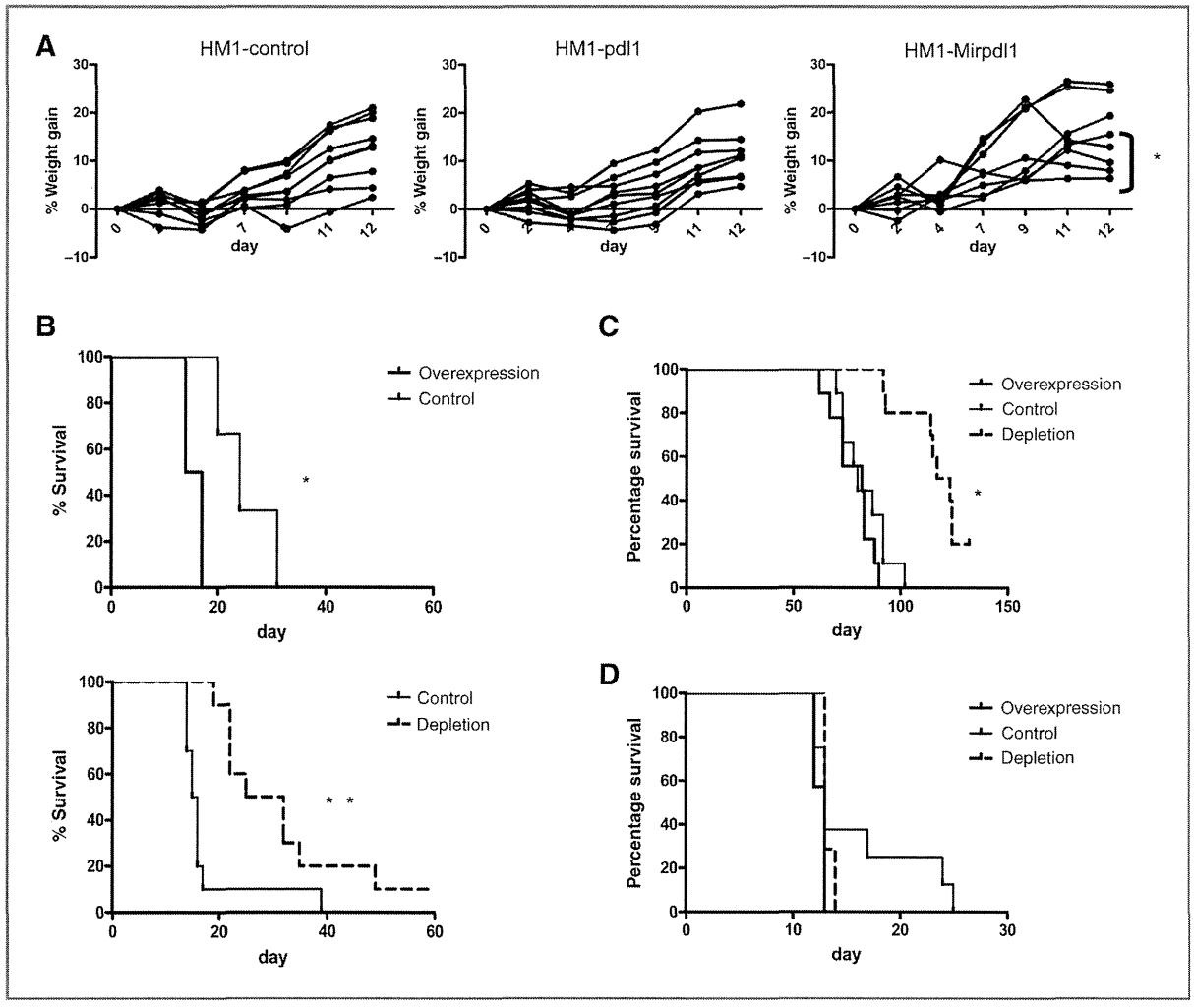

Figure 6. PD-L1 depletion prevents tumor progression and prolongs mouse survival. A, mouse body weight gain is plotted after intraperitoneal injection of HM1-control (left), HM1-pdl1 (middle), or HM1-Mirpdl1 (right). Weight is a reliable marker of tumor growth. Body weight decreased in 4 of 8 mice in HM1-Mirpdl1 group (*). B, survival of HM1-pdl1–injected mice (thick line) and HM1-control–injected mice (thin line); *, $P = 0.039$ ($n = 5$; top), and survival of HM1-control–injected mice (thin line) and HM1-Mirpdl1-injected mice (dotted line); **, $P = 0.0029$ ($n = 10$; bottom). C, survival of ID8-pdl1–injected mice (thick line), ID8-control–injected mice (thin line), and ID8-Mirpdl1–injected mice (dotted line). ID8-control versus ID8-Mirpdl1; *, $P < 0.001$ ($n = 10$). D, survival of SCID mice intraperitoneally injected with HM1-pdl1 (thick line), HM1-control (thin line), and HM1-Mirpdl1 (dotted line). Differences between the groups are not significant ($n = 10$).

mouse peritoneal cavity, whereas IFN-γ concentration in ascites supernatant was too low to induce PD-L1 expression. However, flow cytometric analysis of ascites cells indicated that there are numerous T lymphocytes positive for intracellular IFN-γ, and coincubation with ascites cells, ascites $CD8^+$ lymphocytes, or *in vitro* activated spleen-derived lymphocytes induced PD-L1 on ovarian cancer cells, whereas hypoxic condition or floating culture did not. Notably, HM-1 cells did not express PD-L1 in SCID mouse ascites, suggesting that the copresence of lymphocytes is required for the induction of PD-L1. Taken together, our study indicates that type B cancer cells begin to express PD-L1 when they encounter activated lymphocytes in ascites. Although precise mechanism to explain the difference in PD-L1 expression is not fully understood, there are several reports showing that PD-L1 is overexpressed under influence of oncogenic mutation such as PTEN loss (37) or NPM/ALK (38), which might be the case in type A tumors. On the other hand, type C tumors, which do not respond to IFN-γ, may have some impairment in IFN-receptors or its downstream signals. Namely, tumor cells express PD-L1 depending on both the cell nature (types A, B, or C) and its immune microenvironment. Therefore, in selecting the patients for PD-L1–targeted therapy in ovarian cancer, it might be necessary to assess not only the PD-L1 status of the primary tumor but also the PD-L1 and immune status in the ascites, to predict whether the case will be sensitive to the therapy or not.

Published OnlineFirst January 22, 2013; DOI: 10.1158/1078-0432.CCR-12-2199

Next, we generated PD-L1–overexpressing and PD-L1–depleted cell lines, which are representative of types A and C tumor cells, respectively. PD-L1 manipulation did not affect cell proliferation *in vitro*. In contrast, the *in vivo* proliferation of both the rapid- and slow-growing mouse ovarian cancer cell lines, HM-1 and ID8, was markedly affected, suggesting that PD-L1 has an important role in cancer spreading into the peritoneal cavity. There are several reports about immune responses in ascites and peritoneal dissemination (4, 39). In malignant ascites, abundant activated lymphocytes are found. These lymphocytes can easily attack tumor cells, so surviving in ascites should be difficult for tumor cells (9). In our mouse model, there were numerous IFN-γ–producing activated lymphocytes in the ascites. Nonetheless, the PD-L1–expressing tumor cells progressed. In contrast, the progression of PD-L1–depleted tumor cells was inhibited in this environment. The difference between the 2 groups was observed 10 days after inoculating with tumor cells, indicating that the difference is not due to tumor proliferation itself or an innate immune response but rather is due to an adapted immune response. Survival of SCID mouse was not affected by tumor PD-L1, indicating that the difference is due to interaction between PD-L1 and lymphocytes.

There is some controversy about how and in which phase PD-L1 works in tumor immunity. Dong and colleagues reported that tumor-associated PD-L1 promotes T-cell apoptosis but does not alter CTL cytolysis (31). Hirano and colleagues reported that PD-L1 on tumor cells forms a molecular shield to prevent destruction by CTLs without impairing CTL function (40). In contrast, Blank and colleagues reported that PD-L1 inhibits the effector phase of tumor rejection and alters target cell lysis by $CD8^+$ T cells (41). To further elucidate these possibilities, we conducted several *in vitro* assays to evaluate CTL activity against ovarian cancer cells with varying PD-L1 status. A cytotoxicity assay revealed that PD-L1 expression on ID8 cells inhibits the antigen-specific cytolysis by CTLs. The assessment of CD107a expression on CTL surface indicated that CTL degranulation following encounter with PD-L1–overexpressing ID8 cells is significantly suppressed. These data clearly suggest that PD-L1 attenuate CTL activity in effector phase. A time-lapse analysis revealed that gathering of the CTLs to the target tumor cells was markedly inhibited and CTLs behaved as if they ignored tumor cells when the tumor cells overexpressed PD-L1. We also conducted microarray analysis to elucidate the influence of PD-L1 stimuli on gene expression of CTLs. Altered gene profiles of mouse CTLs caused by PD-L1–expressing ovarian cancer cells was significantly coincident with a gene signature associated with human CTL exhaustion (30). These data collectively indicate that, in both human and mouse peritoneal dissemination, PD-L1 induces peripheral tolerance in CTLs and enables tumor cells to evade from the immune system in the peritoneal cavity.

In summary, our study showed for the first time the close relationships between PD-L1 and peritoneal dissemination of cancer cells. PD-L1 expression and peritoneal positive cytology showed a significant correlation in patients with ovarian cancer, and silencing PD-L1 suppressed tumor progression in the mouse peritoneal cavity and prolonged mouse survival. Our data indicate that restoring immune function by inhibiting PD-L1/PD-1 pathway may serve as a promising strategy for controlling the peritoneal dissemination of malignant tumors, including ovarian cancer.

Disclosure of Potential Conflicts of Interest

No potential conflicts of interest were disclosed.

Authors' Contributions

Conception and design: K. Abiko, M. Mandai, J. Hamanishi
Development of methodology: K. Abiko, M. Mandai, J. Hamanishi
Acquisition of data (provided animals, acquired and managed patients, provided facilities, etc.): K. Abiko, M. Mandai, R. Murakami, A. Yamamoto
Analysis and interpretation of data (e.g., statistical analysis, biostatistics, computational analysis): K. Abiko, N. Matsumura, T. Baba, K. Yamaguchi, R. Murakami
Writing, review, and/or revision of the manuscript: K. Abiko, M. Mandai, N. Matsumura, K. Kosaka
Administrative, technical, or material support (i.e., reporting or organizing data, constructing databases): K. Abiko, J. Hamanishi, Y. Yoshioka, T. Baba, B. Kharma
Study supervision: T. Baba, I. Konishi

Acknowledgments

The authors thank Yuko Hosoe and Maki Kurokawa for their excellent technical assistance and Gyohei Egawa for his support.

The costs of publication of this article were defrayed in part by the payment of page charges. This article must therefore be hereby marked *advertisement* in accordance with 18 U.S.C. Section 1734 solely to indicate this fact.

Received July 23, 2012; revised October 18, 2012; accepted December 14, 2012; published OnlineFirst January 22, 2013.

References

1. Roett MA, Evans P. Ovarian cancer: an overview. Am Fam Physician 2009;80:609–16.
2. du Bois A, Reuss A, Pujade-Lauraine E, Harter P, Ray-Coquard I, Pfisterer J. Role of surgical outcome as prognostic factor in advanced epithelial ovarian cancer: a combined exploratory analysis of 3 prospectively randomized phase 3 multicenter trials: by the Arbeitsgemeinschaft Gynaekologische Onkologie Studiengruppe Ovarialkarzinom (AGO-OVAR) and the Groupe d'Investigateurs d'Investigateurs Nationaux Pour les Etudes des Cancers de l'Ovaire l'Ovaire (GINECO). Cancer 2009;115:1234–44.
3. Bookman MA. Developmental chemotherapy and management of recurrent ovarian cancer. J Clin Oncol 2003;21(10 Suppl): 149s–67s.
4. Tan DS, Agarwal R, Kaye SB. Mechanisms of transcoelomic metastasis in ovarian cancer. Lancet Oncol 2006;7:925–34.
5. Padua D, Massague J. Roles of TGFbeta in metastasis. Cell Res 2009;19:89–102.
6. Yoshida J, Horiuchi A, Kikuchi N, Hayashi A, Osada R, Ohira S, et al. Changes in the expression of E-cadherin repressors, Snail, Slug, SIP1, and Twist, in the development and progression of ovarian carcinoma: the important role of Snail in ovarian tumorigenesis and progression. Med Mol Morphol 2009;42:82–91.
7. Yamamura S, Matsumura N, Mandai M, Huang Z, Oura T, Baba T, et al. The activated transforming growth factor-beta signaling pathway in peritoneal metastases is a potential therapeutic target in ovarian cancer. Int J Cancer 2011;130:20–8.

Published OnlineFirst January 22, 2013; DOI: 10.1158/1078-0432.CCR-12-2199

8. Masoumi Moghaddam S, Amini A, Morris DL, Pourgholami MH. Significance of vascular endothelial growth factor in growth and peritoneal dissemination of ovarian cancer. Cancer Metastasis Rev 2012;31:143–62.
9. Peoples GE, Schoof DD, Andrews JV, Goedegebuure PS, Eberlein TJ. T-cell recognition of ovarian cancer. Surgery 1993;114:227–34.
10. Abrahams VM, Straszewski SL, Kamsteeg M, Hanczaruk B, Schwartz PE, Rutherford TJ, et al. Epithelial ovarian cancer cells secrete functional Fas ligand. Cancer Res 2003;63:5573–81.
11. Curiel TJ, Coukos G, Zou L, Alvarez X, Cheng P, Mottram P, et al. Specific recruitment of regulatory T cells in ovarian carcinoma fosters immune privilege and predicts reduced survival. Nat Med 2004;10: 942–9.
12. Gordon IO, Freedman RS. Defective antitumor function of monocyte-derived macrophages from epithelial ovarian cancer patients. Clin Cancer Res 2006;12:1515–24.
13. Hanahan D, Weinberg RA. Hallmarks of cancer: the next generation. Cell 2011;144:646–74.
14. Thibodeaux SR, Curiel TJ. Immune therapy for ovarian cancer: promise and pitfalls. Int Rev Immunol 2011;30:102–19.
15. Hamanishi J, Mandai M, Iwasaki M, Okazaki T, Tanaka Y, Yamaguchi K, et al. Programmed cell death 1 ligand 1 and tumor-infiltrating $CD8^+$ T lymphocytes are prognostic factors of human ovarian cancer. Proc Natl Acad Sci U S A 2007;104:3360–5.
16. Li K, Mandai M, Hamanishi J, Matsumura N, Suzuki A, Yagi H, et al. Clinical significance of the NKG2D ligands, MICA/B and ULBP2 in ovarian cancer: high expression of ULBP2 is an indicator of poor prognosis. Cancer Immunol Immunother 2009;58:641–52.
17. Liu M, Matsumura N, Mandai M, Li K, Yagi H, Baba T, et al. Classification using hierarchical clustering of tumor-infiltrating immune cells identifies poor prognostic ovarian cancers with high levels of COX expression. Mod Pathol 2009;22:373–84.
18. Hamanishi J, Mandai M, Abiko K, Matsumura N, Baba T, Yoshioka Y, et al. The comprehensive assessment of local immune status of ovarian cancer by the clustering of multiple immune factors. Clin Immunol 2011;141:338–47.
19. Dong H, Zhu G, Tamada K, Chen L. B7-H1, a third member of the B7 family, co-stimulates T-cell proliferation and interleukin-10 secretion. Nat Med 1999;5:1365–9.
20. Freeman GJ, Long AJ, Iwai Y, Bourque K, Chernova T, Nishimura H, et al. Engagement of the PD-1 immunoinhibitory receptor by a novel B7 family member leads to negative regulation of lymphocyte activation. J Exp Med 2000;192:1027–34.
21. Brahmer JR, Drake CG, Wollner I, Powderly JD, Picus J, Sharfman WH, et al. Phase I study of single-agent anti-programmed death-1 (MDX-1106) in refractory solid tumors: safety, clinical activity, pharmacodynamics, and immunologic correlates. J Clin Oncol 2010;28:3167–75.
22. Topalian SL, Hodi FS, Brahmer JR, Gettinger SN, Smith DC, McDermott DF, et al. Safety, activity, and immune correlates of anti-PD-1 antibody in cancer. N Engl J Med 2012;366:2443–54.
23. Brahmer JR, Tykodi SS, Chow LQ, Hwu WJ, Topalian SL, Hwu P, et al. Safety and activity of anti-PD-L1 antibody in patients with advanced cancer. N Engl J Med 2012;366:2455–65.
24. Zheng Q, Wang XJ. GOEAST: a web-based software toolkit for Gene Ontology enrichment analysis. Nucleic Acids Res 2008;36:W358–63.
25. Sana TR, Janatpour MJ, Sathe M, McEvoy LM, McClanahan TK. Microarray analysis of primary endothelial cells challenged with different inflammatory and immune cytokines. Cytokine 2005;29:256–69.
26. Roby KF, Taylor CC, Sweetwood JP, Cheng Y, Pace JL, Tawfik O, et al. Development of a syngeneic mouse model for events related to ovarian cancer. Carcinogenesis 2000;21:585–91.
27. Janát-Amsbury MM, Yockman JW, Anderson ML, Kieback DG, Kim SW. Comparison of ID8 MOSE and VEGF-modified ID8 cell lines in an immunocompetent animal model for human ovarian cancer. Anticancer Res 2006;26:2785–9.
28. Yamaguchi K, Mandai M, Oura T, Matsumura N, Hamanishi J, Baba T, et al. Identification of an ovarian clear cell carcinoma gene signature that reflects inherent disease biology and the carcinogenic processes. Oncogene 2010;29:1741–52.
29. Hamanishi J, Mandai M, Matsumura N, Baba T, Yamaguchi K, Fujii S, et al. Activated local immunity by CC chemokine ligand 19-transduced embryonic endothelial progenitor cells suppresses metastasis of murine ovarian cancer. Stem Cells 2009;28:164–73.
30. Quigley M, Pereyra F, Nilsson B, Porichis F, Fonseca C, Eichbaum Q, et al. Transcriptional analysis of HIV-specific $CD8^+$ T cells shows that PD-1 inhibits T cell function by upregulating BATF. Nat Med 2010;16:1147–51.
31. Dong H, Strome SE, Salomao DR, Tamura H, Hirano F, Flies DB, et al. Tumor-associated B7-H1 promotes T-cell apoptosis: a potential mechanism of immune evasion. Nat Med 2002;8:793–800.
32. Zou W, Chen L. Inhibitory B7-family molecules in the tumour microenvironment. Nat Rev Immunol 2008;8:467–77.
33. Petroff MG, Chen L, Phillips TA, Hunt JS. B7 family molecules: novel immunomodulators at the maternal-fetal interface. Placenta 2002;23 (Suppl A):S95–101.
34. Hori J, Wang M, Miyashita M, Tanemoto K, Takahashi H, Takemori T, et al. B7-H1-induced apoptosis as a mechanism of immune privilege of corneal allografts. J Immunol 2006;177:5928–35.
35. Muhlbauer M, Fleck M, Schutz C, Weiss T, Froh M, Blank C, et al. PD-L1 is induced in hepatocytes by viral infection and by interferon-alpha and -gamma and mediates T cell apoptosis. J Hepatol 2006;45:520–8.
36. Waeckerle-Men Y, Starke A, Wuthrich RP. PD-L1 partially protects renal tubular epithelial cells from the attack of $CD8^+$ cytotoxic T cells. Nephrol Dial Transplant 2007;22:1527–36.
37. Parsa AT, Waldron JS, Panner A, Crane CA, Parney IF, Barry JJ, et al. Loss of tumor suppressor PTEN function increases B7-H1 expression and immunoresistance in glioma. Nat Med 2007;13:84–8.
38. Marzec M, Zhang Q, Goradia A, Raghunath PN, Liu X, Paessler M, et al. Oncogenic kinase NPM/ALK induces through STAT3 expression of immunosuppressive protein CD274 (PD-L1, B7-H1). Proc Natl Acad Sci U S A 2008;105:20852–7.
39. Aslam N, Marino CR. Malignant ascites: new concepts in pathophysiology, diagnosis, and management. Arch Intern Med 2001;161: 2733–7.
40. Hirano F, Kaneko K, Tamura H, Dong H, Wang S, Ichikawa M, et al. Blockade of B7-H1 and PD-1 by monoclonal antibodies potentiates cancer therapeutic immunity. Cancer Res 2005;65:1089–96.
41. Blank C, Brown I, Peterson AC, Spiotto M, Iwai Y, Honjo T, et al. PD-L1/B7H-1 inhibits the effector phase of tumor rejection by T cell receptor (TCR) transgenic $CD8^+$ T cells. Cancer Res 2004;64:1140–5.

Huang et al. BMC Medical Genomics 2012, 5:47
http://www.biomedcentral.com/1755-8794/5/47

BMC Medical Genomics

RESEARCH ARTICLE Open Access

Histotype-specific copy-number alterations in ovarian cancer

Ruby YunJu Huang[1,2†], Geng Bo Chen[3†], Noriomi Matsumura[4], Hung-Cheng Lai[5], Seiichi Mori[2], Jingjing Li[3], Meng Kang Wong[2], Ikuo Konishi[4], Jean-Paul Thiery[2,6] and Liang Goh[3,7,8*†]

Abstract

Background: Epithelial ovarian cancer is characterized by multiple genomic alterations; most are passenger alterations which do not confer tumor growth. Like many cancers, it is a heterogeneous disease and can be broadly categorized into 4 main histotypes of clear cell, endometrioid, mucinous, and serous. To date, histotype-specific copy number alterations have been difficult to elucidate. The difficulty lies in having sufficient sample size in each histotype for statistical analyses.

Methods: To dissect the heterogeneity of ovarian cancer and identify histotype-specific alterations, we used an *in silico* hypothesis-driven approach on multiple datasets of epithelial ovarian cancer.

Results: In concordance with previous studies on global copy number alterations landscape, the study showed similar alterations. However, when the landscape was de-convoluted into histotypes, distinct alterations were observed. We report here significant histotype-specific copy number alterations in ovarian cancer and showed that there is genomic diversity amongst the histotypes. 76 cancer genes were found to be significantly altered with several as potential copy number drivers, including ERBB2 in mucinous, and TPM3 in endometrioid histotypes. ERBB2 was found to have preferential alterations, where it was amplified in mucinous (28.6%) but deleted in serous tumors (15.1%). Validation of ERBB2 expression showed significant correlation with microarray data (p=0.007). There also appeared to be reciprocal relationship between KRAS mutation and copy number alterations. In mucinous tumors where KRAS mutation is common, the gene was not significantly altered. However, KRAS was significantly amplified in serous tumors where mutations are rare in high grade tumors.

Conclusions: The study demonstrates that the copy number landscape is specific to the histotypes and identification of these alterations can pave the way for targeted drug therapy specific to the histotypes.

Keywords: Ovarian cancer, Histological biomarkers, Genomics, Copy number driver genes, ERBB2

Background

Ovarian cancer is often dubbed a 'silent' killer because of its non-specific symptoms and late clinical onset which contribute to overall poor prognosis. There has been a steady increase in incidence over the last three decades with 204,000 new cases diagnosed each year globally [1]. It ranked fifth in mortality among cancers in women and has the highest case-fatality rate in gynecological cancers [2]. The 5-year survival rate for women with advanced disease remains at 29% with estimated 125,000 deaths annually [1,3].

About 90% ovarian cancers are epithelial ovarian cancer (EOC) [4], histologically subtyped as serous, mucinous, endometrioid, or clear cell. Further subtyping include the borderline cases, such as mucinous or serous borderline, often presented as stable diseases with more favorable outcome compared to the non-borderline subtypes. It is now recognized that epithelial ovarian cancer is a spectrum of diseases with varied genetic mutations among histotypes [5]. Genetically, mutations differ between the grades of the disease. Low-grade serous carcinoma have high frequency of KRAS and BRAF mutations but few p53 mutations

* Correspondence: liang.goh@duke-nus.edu.sg
†Equal contributors
[3]Cancer & Stem Cell Biology, Duke-National University of Singapore Graduate Medical School, 8 College road, Rm 6-32, Singapore 169857, Singapore
[7]Department of Medical Oncology, National Cancer Centre Singapore, 11 Hospital Drive, Singapore 169610, Singapore
Full list of author information is available at the end of the article

while high grade serous carcinoma shows the inverse in frequency of these mutations [6,7]. Mucinous histotype has KRAS mutations [8] and endometrioid has PTEN mutations [9]. Despite the molecular heterogeneity, the treatment standard remains as taxane/platinum-based chemotherapy for all histotypes.

Genomic alterations such as copy number alterations (CNA) have been known to harbor drivers in carcinogenesis. Driver genes are genes that confer growth advantage on the cancer cells [10]. Several known copy number alteration drivers in cancers include receptor tyrosine kinases such as EGFR, FGFR, and ERBB2, which are targets for drugs therapy [11]. Successful incorporation of genomics alterations studies in cancer treatment has been evident in breast, leukemia, and lung cancers, where targeted therapies are part of the standard treatment protocols [12-14]. For example, Trastuzumab, a targeted therapy that can significantly reduce risk of disease recurrence and improve overall survival, is now standard of care for early-stage patients with Her2-positive breast cancer [14]. To date, targeted drug therapy has not been successfully incorporated in EOC.

One of the challenges in elucidating copy number alterations in EOC is the disproportional prevalence of histotype. Serous is the most prevalent (70-85%), followed by endometrioid (5-10%), clear cell (5-10%), and mucinous (~5%). The lower prevalent diseases tend to suffer from small sample size for statistical analyses to identify copy number alterations. To elucidate CNA in each histotype, we combined data from multiple studies with similar platforms to identify copy number alterations that are specific to the histotypes. The motivation is to identify high confidence histotype-specific alterations that may otherwise be obscured due to disproportionate prevalence of the histotypes.

Results

Two major results are presented here; the histotype-specific copy number alterations for EOC and the identification of potential driver genes. Three datasets with corresponding gene expression and copy number profiling on similar platforms were used for this study. A hypothesis-driven approach using stringent false discovery rate (FDR) filtering was used to identify potential copy number driver genes (Methods). The genes were compared with other studies as well as cancer genes reported in literature. In addition, we also validated the expression of ERBB2, a driver gene, via quantitative real-time PCR (qPCR).

Distinct copy number alterations in EOC histotypes

Figure 1a shows the global frequency of copy number aberrations for EOC across the genome for the merged dataset. In concordance with other reports, the four commonly reported chromosomes of 3q, 8, 17p, and 20q showed broad copy number alterations in EOC [15-17]. When this was de-convoluted into histotypes (Figure 1b, shown in 4 tracks for clear cell, endometrioid, mucinous, and serous), distinct differences were observed. It is evident that the general frequency for EOC was mirrored in serous tumors, not surprising since it has the largest sample size. In the four most commonly reported altered regions, 3q, 8, and 20q amplifications were observed in serous, clear cell, endometrioid but not mucinous tumors. Endometrioid and serous tend to harbor more copy number alterations, with more broad regions of alterations involving the p- or q-arm. The genomics landscape for clear cell and mucinous tumors appeared different from the other histotypes, with lesser broad regions of alterations and in lower frequency.

To assess the significance of copy number altered regions, we used a 2-pronged approach using merged and individual datasets (Additional file 1: Figure S1). Figure 2 shows significant copy number altered regions (see Methods) in the histotypes. Broad 3p amplification and 8p deletion were observed in serous tumors; 8q amplifications in clear cell and serous tumors; 17p deletions in mucinous and serous tumors; and chr20 amplifications in serous tumors. The nature of the alterations also differs, e.g. focal versus broad alterations. For example in 3q, serous tumors showed broader amplifications in the region of 3q13.31-29 while focal amplification was observed for clear cell tumors at 3q26.2-26.32. This is interesting as it has been reported that overlapping broad and focal aberrations can have distinct functional consequences [18]. In other chromosomes, alterations were specific to histotypes as well; such as 9p21 focal deletions in mucinous histotype, reportedly harboring homozygous deletions in EOC [19-22]. There are regions that displayed opposite trend in alterations between histotypes. One particular region, 8p23.1, showed amplification in clear cell but deletion in serous tumors. Another region which showed opposite trend in alteration was 17q12 which harbor the oncogene ERBB2; the gene was significantly amplified in mucinous but deleted in serous tumors. Excluding borderline cases, 28.6% (4/14) mucinous samples had amplifications and 15.2% (15/99) of serous tumors had deletions of ERBB2. 1/5 mucinous borderline also showed ERBB2 amplification. It should be of note that although ERBB2 was found significantly deleted in serous tumors, 5/99 (5.1%) of serous samples harbored the amplification, close to the 3% reported by TCGA for high grade serous [23]. No ERBB2 deletion was observed in the mucinous samples. As serous tumors have a comparatively larger sample size than the other histotypes, we would expect more significant regions for this histotype. Nevertheless, using stringent criteria, we were able to identify some significant CNA for the lower prevalent tumors.

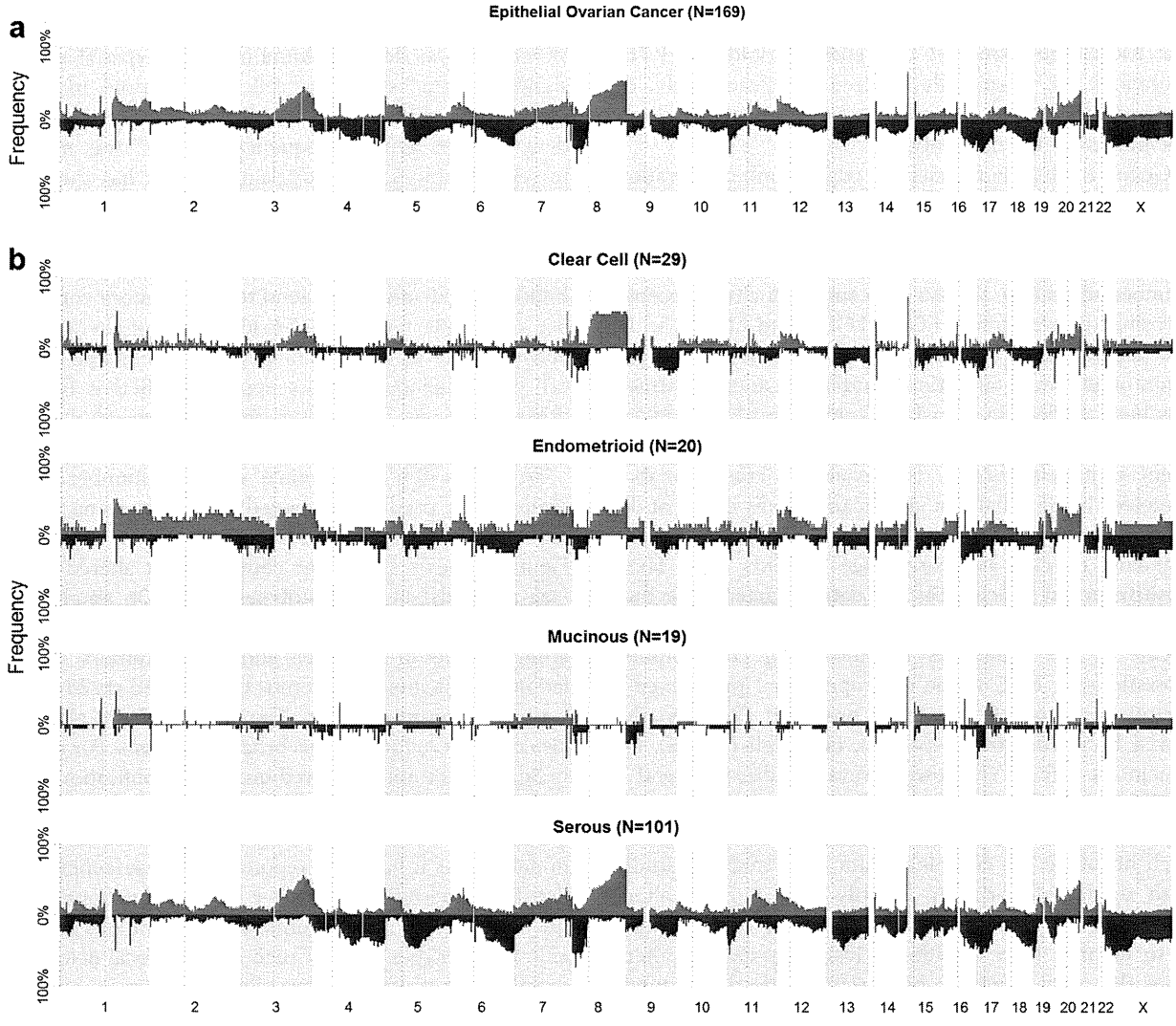

Figure 1 Overview of copy number aberrations in EOC from 3 datasets from chromosomes 1-X. Chromosomes are shown in alternating blocks of grey. The centromere for each chromosome is shown as a dotted line. (**a**) Frequency (%) of occurrence of amplification (red) and deletion (blue) from chromosome 1 to X in epithelial ovarian cancer from the merged 3 datasets. Major regions of alterations reported in other studies are similarly observed: e.g. chr 3, 8, 17, and 20. (**b**) Frequency (%) of occurrence in the 4 main histotypes of EOC. Threshold for frequency was set at LRR ≥ |0.2|. The frequency for serous tumors is similar to that in (**a**). However, frequency for the lower prevalent histotypes showed evident differences, indicating the molecular differences between the histotypes.

To quantify genes that were altered in each histotype, we mapped genes to regions that were identified in each histotype. 6375 unique genes were found to be altered: 2682 amplifications and 3712 deletions (Additional file 2: Table S1). 91% of genes were amplified and 97.1% deleted in serous tumors, 19.1% amplified and 1.5% deleted in clear cell, 14.3% amplified in endometrioid, and 0.5% amplified and 11.5% deleted in mucinous. A total of 5360 genes were specific to each histotype (amplification=2014, deletion=3346), 5011 in serous tumors, 193 in endometrioid tumors, 79 in clear cell tumors, and 77 in mucinous tumors. Within each histotype, the type of alterations varied. Clear cell tumors had more amplified genes than deleted genes, while mucinous and serous tumors had more deleted genes than amplified genes. Only amplified genes were found in endometrioid tumors. Figure 3 shows the Venn diagram of overlapping genes in the lower prevalent histotypes. Due to the differences in sample size of each histotype, comparisons between overlapped genes were limited to genes found only in the non-serous tumors where the sample sizes are more comparable. A small number of overlapped amplified and deleted genes between clear cell and mucinous tumors were observed; none with endometrioid. This suggests that most of the